Marrow stromal cells form guiding strands in the injured spinal cord and promote recovery

C. P. Hofstetter*, E. J. Schwarz†, D. Hess*, J. Widenfalk*, A. El Manira*, Darwin J. Prockop††, and L. Olson*

*Department of Neuroscience, Karolinska Institutet, S-171 77 Stockholm, Sweden; and †Center for Gene Therapy, Tulane University Health Sciences Center, New Orleans, LA 70112

Marrow stromal cells (MSC) can be expanded rapidly *in vitro* and differentiated into multiple mesodermal cell types. In addition, differentiation into neuron-like cells expressing markers typical for mature neurons has been reported. To analyze whether such cells, exposed to differentiation media, could develop electrophysiological properties characteristic of neurons, we performed whole-cell recordings. Neuron-like MSC, however, lacked voltage-gated ion channels necessary for generation of action potentials. We then delivered MSC into the injured spinal cord to study the fate of transplanted MSC and possible effects on functional outcome in animals rendered paraplegic. MSC given 1 week after injury led to significantly larger numbers of surviving cells than immediate treatment and significant improvements of gait. Histology 5 weeks after spinal cord injury revealed that MSC were tightly associated with longitudinally arranged immature astrocytes and formed bundles bridging the epicenter of the injury. Robust bundles of neurofilament-positive fibers and some 5-hydroxytryptamine-positive fibers were found mainly at the interface between graft and scar tissue. MSC constitute an easily accessible, easily expandable source of cells that may prove useful in the establishment of spinal cord repair protocols.

Most, if not all, central nervous system neurons in mammals have the intrinsic capacity to regenerate a lost axon. The failure of axons to regenerate after spinal cord injury (SCI) has been attributed to growth-inhibitory molecules (1), lack of appropriate trophic support (2, 3), and reactions of the immune system (4). Glial cells produce growth-inhibiting molecules, such as Nogo (5, 6), MAG (7), tenascin (8), and chondroitin sulfate proteoglycans (9). Up-regulation of neurotrophic factors after SCI is limited (3). The role of the immune system in SCI is complex but may include nerve growth inhibitory as well as stimulatory events (4, 10). Davies *et al.* (11) demonstrated long-distance regeneration of adult dorsal root ganglion cells, transplanted into spinal cord pathways, if a micrografting technique was used to avoid local scarring. However, axon outgrowth was terminated or reversed upon contact with scar tissue. One approach to overcome some of the growth-inhibiting properties of the injured spinal cord is to transplant cells with protective and/or reparative properties to the site of injury. Recently, mouse embryonic stem cells, delivered into the injured spinal cord, were shown to differentiate into neurons, astrocytes, and oligodendrocytes and to improve motor function (12). However, recovery was limited. Also, the use of embryonic stem cells may not be generally accepted and heterologous transplantation may elicit graft rejection. Marrow stromal cells (MSC) constitute an alternative source of pluripotent stem cells. Under physiological conditions, they are believed to maintain the architecture of bone marrow and regulate hematopoiesis with the help of different cell-adhesion molecules and the secretion of cytokines, respectively (13). MSC grown out of bone marrow cell suspensions by their selective attachment to tissue culture plastic can be expanded efficiently (14, 15) and manipulated genetically (16). MSC are referred to as mesenchymal stem cells because they are capable of differentiating into multiple mesodermal tissues, including bone (17), cartilage (18), fat (17), and muscle (19). In

addition, differentiation into neuron-like cells expressing neuronal markers has been reported (20–22), suggesting that MSC may be capable of overcoming germ layer commitment. Importantly, MSC can migrate along known migration pathways when injected into corpus striatum of rats (14). MSC migrated throughout forebrain and cerebellum, integrated into central nervous system cytoarchitecture, and expressed markers typical of mature astrocytes and neurons after injection into the lateral ventricle of neonatal mice (23).

We examined whether MSC expressing neuronal markers *in vitro* exhibited physiological properties characteristic of neurons. We then delivered MSC into the injured spinal cord to monitor survival, spread and differentiation of such cells, and their possible effects on the motor behavior of rats rendered paraplegic by SCI.

Methods

Primary Marrow Stromal Cell Cultures. MSC were collected from femurs and tibias of adult male Lewis rats (Harlan Breeders, Indianapolis) (16). Rats were euthanized with a mixture of 70% CO_2 and 30% O_2. Tibias and femurs were placed on ice in MEM with alpha modification (α-MEM; GIBCO/BRL) containing 20% FCS (Atlanta Biologicals, Norcross, GA), 2 mM L-glutamine (GIBCO/BRL), 100 units/ml penicillin, 100 μg/ml streptomycin, and 25 ng/ml amphotericin B (penicillin, streptomycin, and amphotericin; GIBCO/BRL). Epiphyses of femurs and tibias were removed, and the marrow was flushed out by using a syringe filled with medium. Bone marrow was filtered through a 70-μm nylon mesh and plated in 75-cm^2 flasks. About 24 h after plating, supernatant containing nonadherent cells was removed and fresh medium was added. After the cells had grown to near confluency, they were passaged two to five times by being detached (0.25% trypsin/1 mM EDTA for 5 min) and replated at a density of $\approx$5,000 cells/cm^2.

Preparation of the Retroviral Vector, Production of Viral Particles, and Genetic Marking of MSC. A retroviral construct encoding green fluorescent protein (GFP) as an expression marker and aminoglycoside phosphotransferase as a neomycin (G418) selectable marker was prepared by using the LXSN vector (CLONTECH) (24). Phoenix amphotropic packaging cells (25) (ATCC) were transfected with the LXSN-GFP plasmid by using calcium phosphate precipitation. Viral supernatants were collected 48 h after the start of the transfection, filtered through a 0.45-μm filter, and stored at -80°C for further use. Phoenix packaging cells were analyzed at the time of viral harvest for GFP expression. One day before the infection of MSC with GFP-retrovirus, about 100,000 MSC were plated in 21.0-cm^2 plates. At the time

---

of infection, defined as day 1, 2.5 ml of complete medium containing 20% heat-inactivated FCS was added to the cells in the presence of 500 μl of viral supernatant and 8 μg/ml polybrene (Sigma). On day 2, the infection procedure was repeated. On day 3, fresh complete medium was added with 20% FCS (not heat-inactivated). On day 4, cells were split 1:3 in 55.0-cm^2 plates in complete medium containing 200 μg/ml G418 (Sigma) for a selection period of 14–21 days. MSC that had stably integrated the transgene survived and were expanded for experiments by passaging cells three to nine times.

Attempts at Differentiation of MSC Toward a Neuronal Fate. MSC were plated as described (20) at a density of 2,500 cells/cm^2. On the following day, the medium was replaced with preinduction medium consisting of DMEM (Sigma), 20% FCS, and 10 ng/ml basic fibroblast growth factor. After 24 h, the preinduction medium was removed, the cells were washed twice with PBS, and neuronal induction medium containing DMEM supplemented with 2% DMSO and 200 μm butylated hydroxyanisole (20) was added. In later experiments, we used DMEM with 5 mM 2-mercaptoethanol (20) as an alternative neuronal induction medium for the same incubation times.

Electrophysiological Recordings of Neuron-Like MSC. Whole-cell recordings were made of MSC exhibiting possible neuronal morphologies such as rounded cell bodies and distinct processes with growth cone-like terminal expansions. Such differentiated cells will be referred to as neuron-like MSC. Whole-cell recordings were obtained by using a patch-clamp amplifier (Axopatch 200 A; Axon Instruments). The recordings had a series resistance ranging from 4 to 10 MΩ that was compensated for electronically by 75–85%. The resting membrane potential was assessed in current clamp mode. The residual capacity was removed, but the linear leak was not subtracted. To investigate the existence of voltage-gated channels, neuron-like MSC were clamped at -120 mV and currents were evoked by 100-ms depolarizing voltage steps to $+30$ mV. The cells were perfused through a gravity-driven microperfusion system with the nozzle positioned close to the recorded cell. The control solution was used at room temperature and contained 140 mM NaCl, 4 mM KCl, 1.8 mM CaCl$_2$, 1 mM MgCl$_2$, 23 mM sucrose, and 10 mM Hepes. The pH was adjusted to 7.40; the osmolarity, to 310 mosM. Recordings were made with pipettes of 3–7 MΩ filled with a solution containing 4 mM NaCl, 140 mM KCl, 0.5 mM CaCl$_2$, 1 mM MgCl$_2$, 10 mM Hepes, and 5 mM EGTA. The pH was adjusted to 7.40; the osmolarity, to 305 mosM. Membrane currents and voltages were controlled with appropriate software (PCLAMP; Axon Instruments). Current and voltage signals were sampled at 10 kHz.

MSC Transplantation Into the Injured Spinal Cord. A total of 38 adult female Lewis rats (Charles River Breeding Laboratories) weighting 250–260 g received a standardized contusion of the spinal cord and MSC treatment immediately or 1 week after injury. Laminectomy was performed at T9 under halothane anesthesia (Fluothane; AstraZeneca Södertälje, Sweden). The impact rod of the NYU device (26) was centered above T9 and dropped from a height of 25 mm. MSC grown under normal culture conditions were detached and resuspended with α-MEM to a final concentration of 30,000 viable cells/μl as determined by trypan blue dye exclusion. Immediately, or 7 days after injury, animals received 5 μl of a MSC suspension or α-MEM delivered into the injury center and two 2.5-μl deposits, one 2-mm cranial, and the other 2-mm caudal of the central injection. A total of 300,000 cells or vehicle thus was delivered at a rate of 0.5 μl per minute by means of a stereotaxic frame and a glass pipette with a tip diameter of 100 μm configured to a 10-μl Hamilton syringe. Muscle and skin were sutured separately. Urinary bladders were emptied manually five times per day for the first week and twice daily thereafter. Antibiotics (Borgal; Hoechst Pharmaceuticals) were given to prevent urinary tract infection. Two independent experiments with time-matched controls were carried out. A total of 16 rats received MSC ($n = 8$) or cell culture medium ($n = 8$) immediately after injury. A second group ($n = 22$) was treated with MSC ($n = 12$) or vehicle ($n = 10$) 1 week after injury. In both groups, behavior was assessed on a weekly basis, and histological examinations were carried out on animals euthanized 5 weeks after injury. All experiments had been approved by the Animal Research Committee of Stockholm.

Behavioral Testing. Hindlimb motor function was assessed by using the open-field BBB scoring system (27). Individual rats were placed on an open field (75 $\times$ 125 cm) and observed for 4 min by two observers. Hindlimb function was scored from 0 to 21 (flaccid paralysis to normal gait). The test was carried out 1 day postoperatively and once every week up to the fifth week after SCI.

Cell Quantification. GFP-positive cell profiles containing a distinct nucleus were counted in serial sections. Cell numbers were calculated according to the formula of Abercrombie (28).

Immunocytochemistry. Tissues and cells were processed for indirect immunocytochemistry (29). Animals were deeply anesthetized (Pentobarbital) and perfused intracardially with 50 ml of Tyrode's solution containing 0.1 ml of Heparin, followed by 200 ml of fixative (4% paraformaldehyde/0.4% picric acid in PBS). Spinal cords were dissected, postfixed in similar fixative for 1 hour, transferred to 10% sucrose solution, frozen, and cut in a cryostat at 14-μm thickness. Longitudinal sections were collected from 18-mm-long spinal cord segments containing the injury and injection sites and thaw-mounted on gelatin-coated slides. MSC were grown in chamber slides (Lab-Tek; Nunc) and fixed with 4% paraformaldehyde for 10 min. Antisera raised in goats against fibronectin (Calbiochem) and GFP (Rockland, Gilbertsville, PA) or in rabbits against nestin (kindly provided by Urban Lendahl, Karolinska Institute), laminin (Sigma), GFAP (Sigma), neurofilament (NF; Dahl, Chesnut Hill, MA) (30), PGP 9.5 (Biogenesis, Bournemouth, U.K.), GFP (Molecular Probes), and 5-hydroxytryptamine (5-HT) (Sigma) as well as mouse mAbs to vimentin (Dako), NeuN (Chemicon), NF-200 (Sigma), and Map-2 (Sigma) were used. Secondary antisera were conjugated with FITC, rhodamine, or Cy5 (Jackson ImmunoResearch). Optimal dilutions were established for all primary and secondary antibodies. Controls included omitting the primary antibody. Slides were evaluated by using epifluorescence and confocal microscopy (Radiance 2100; Bio-Rad).

Statistical Analysis. Comparisons of cell survival were made by using an unpaired t test. Between-group comparisons for behavior were carried out by using the Mann–Whitney U test. Significance levels were designated $P < 0.05$, $P < 0.01$, or $P < 0.001$. All values are given as mean $\pm$ SEM.

Results

Labeling and Characterization of MSC in Vitro. Reliable detection by fluorescence microscopy of marrow stromal cells in culture and after transplantation was achieved by transducing MSC with a retrovirus encoding GFP. After a selection time of 14 days in medium supplemented with a cell-toxic concentration of G418, only cells that had permanently integrated plasmids containing a neomycin selectable marker survived. The successful labeling of all surviving cells was confirmed by fluorescence microscopy. Genetically labeled MSC did not alter their morphology compared with native MSC. All analyzed cells ($n > 500$) were positive for fibronectin, vimentin, and laminin (Fig. 1 *A–C* and
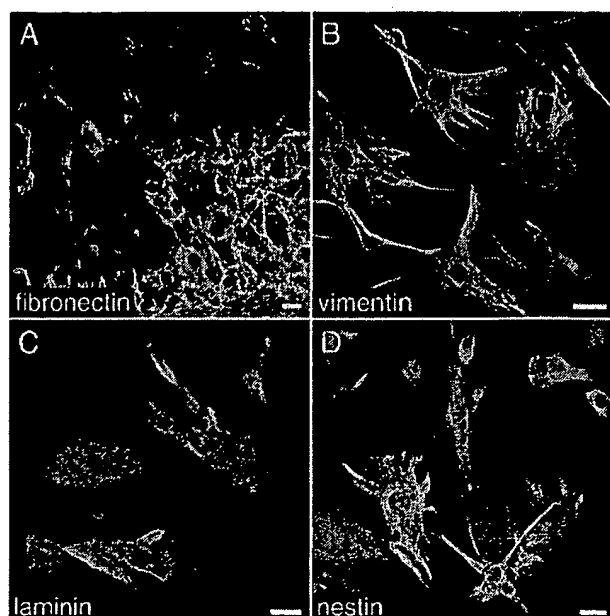
Fig. 1. Appearance of MSC in culture. (A) All MSC display fibronectin-IR during culture conditions. Extensive deposition of fibronectin is observed in the cell cluster in the lower right corner. Vimentin-IR (B) and laminin-IR (C) are expressed by all MSC. (D) Nestin-IR is detected in a subset of MSC with different morphologies. In C and D, the GFP cell marker (green) is shown together with laminin or nestin (red). (Bars = 25 μm.)

Table 1). In areas of high cell density, fibronectin-immunoreactive filaments were deposited extensively in the extracellular space (Fig. 1A). Immunoreactivity (IR) for the mesodermal-intermediate filament vimentin was dense in cellular processes and present in the form of a filamentous meshwork in cell bodies (Fig. 1B). A distinct subpopulation of MSC (37.5% ± 1.2, n = 2,777) was nestin-IR (Fig. 1D). MSC were negative for the neuron-specific markers NeuN, NF, Map-2, and PGP 9.5.

Electrophysiological Properties of Neuron-Like MSC. In one experiment, we induced MSC with medium containing 2% DMSO and 200 μM butylated hydroxyanisole for 48 h (20). However, patch-clamp recordings of these neuron-like MSC were not possible. This could have been a result of changes in the cell membrane caused by dramatic changes in the osmolarity from 646 to 310 mosM when the differentiation medium was replaced by the extracellular solution. In a second experiment, we differentiated MSC with medium containing 5 mM 2-mercaptoethanol for 48 h. This treatment was compatible with whole-cell recordings. The resting membrane potential was −11.4 ± 8.7 mV (n = 8). It was not possible to induce action potentials in any cell by application of depolarizing current

Table 1. IR markers of MSC *in vitro* and after spinal cord implantation

| Marker	MSC *in vitro*	Implanted MSC
Fibronectin	+++	++
Vimentin	++	−
Laminin	+	−
Nestin	++ (37.5% ± 1.2)	−
NeuN	−	+
NF	−	−
GFAP	−	−
Cell shape	Flat	Spindle-shaped

−, No signal; +++, strong signal.
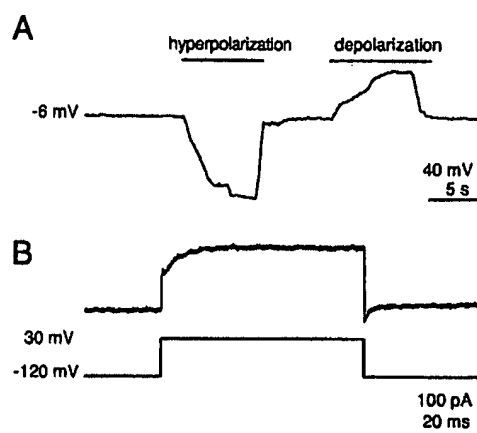
Fig. 2. Electrophysiological properties of a neuron-like MSC. (A) Membrane potential of a neuron-like MSC at rest and during hyperpolarization and depolarization. Note that no action potentials were elicitable even after hyperpolarization to reactivate possible voltage-gated ion channels. (B) Voltage-gated currents elicited via a voltage command stepping from −120 mV to 30 mV. Neither voltage-gated Na$^+$ channels nor voltage-gated K$^+$ channels are present.

(Fig. 2A). By using the voltage step protocol to activate voltage-gated currents, no inward currents could be elicited, indicating that the MSC did not express functional sodium channels. An outward current amplitude was found to be 203 ± 194.5 pA (n = 8) (Fig. 2B). The low amplitude of the outward current and the presence of unavoidable leaks associated with the recording and leak currents make it very unlikely that the observed current represents a voltage-gated, outward potassium current. Hence, MSC differentiated by 2-mercaptoethanol did not show typical neuronal properties such as action potentials or voltage-gated Na$^+$ and K$^+$ currents and, therefore, are not mature neurons.

Delayed Implantation of MSC into the Injured Spinal Cord Improves Functional Recovery. Immediate MSC treatment did not improve locomotor function, as revealed by BBB scoring (Fig. 3A). Delayed implantation led to significantly improved BBB scores (9.2 ± 0.5) compared with sham-grafted animals (7.9 ± 0.1) (Mann–Whitney U test; P = 0.013) (Fig. 3B). Five weeks after injury, control animals could not support their body weight with their hindlimbs (n = 10), whereas seven animals of the treatment
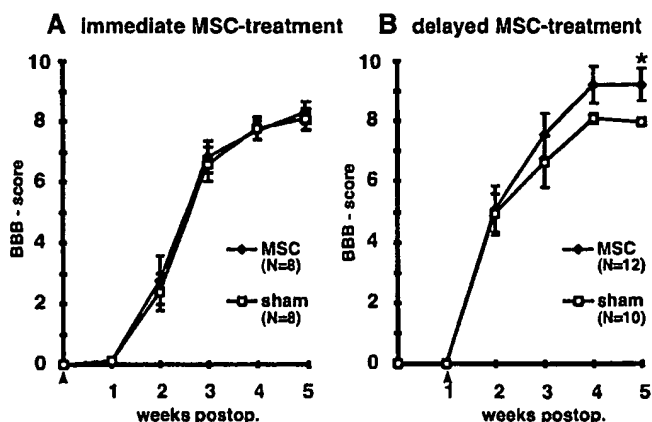

Fig. 3. (A) Analysis of locomotor recovery as measured by BBB scores. Animals treated with MSC immediately after SCI do not differ from control animals. (B) Delayed MSC treatment significantly improved locomotor recovery. *, P = 0.013. Data represent means ± SEM. Arrowheads indicate the treatment time.
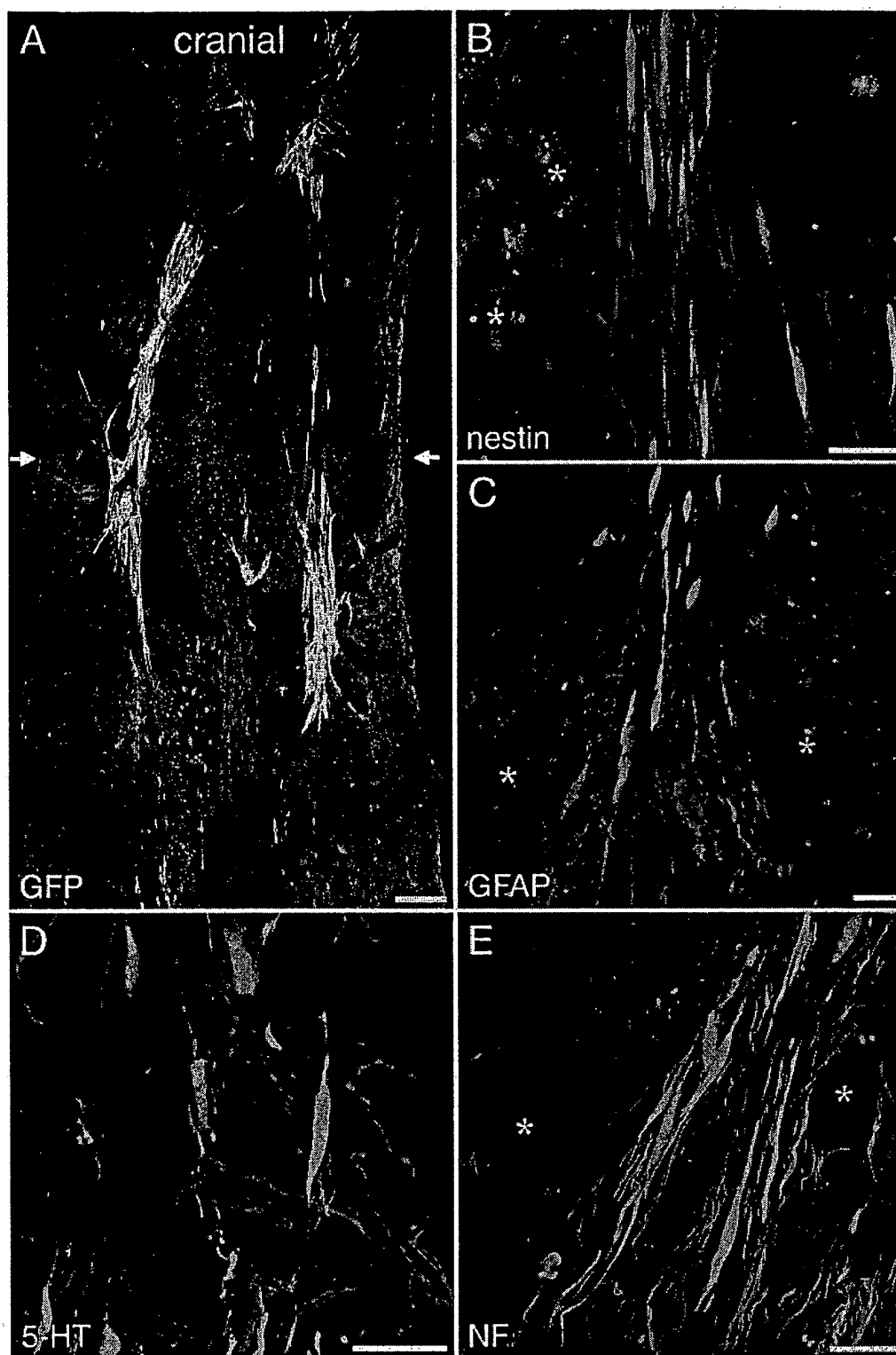
Fig. 4. One-week-delayed transplantation of MSC after SCI. (A) MSC form bundles bridging the epicenter of the lesion visualized by the transgenic GFP marker. Arrows indicate the location of the impact injury. (B) Nestin-immunoreactive immature astrocytes with longitudinally aligned processes (red) are found within MSC bundles (green). (C) GFAP-IR (red) marks astrocytic processes penetrating the grafted cell aggregates (green). (D) 5-HT-positive fibers (red) are present among the implanted MSC (green). (E) Robust NF-IR nerve fiber bundles (red) are found at the interface between MSC and host tissue. (B, C, and E) Asterisks indicate macrophages. [Bars = 250 μm (A) and 25 μm (B–E).]

group ($n = 12$) could lift their trunks and two of them regained stepping patterns with bilateral weight support and frequent forelimb–hindlimb coordination assessed as 13 on the BBB scale. Cryostat sections were examined 5 weeks after SCI. MSC were detected reliably by their GFP labeling, which was abundant in the whole cell body. Cell counts revealed significantly larger numbers of cells (2,966 ± 681, $n = 8$) in animals treated 1 week after injury than in animals treated immediately (518 ±
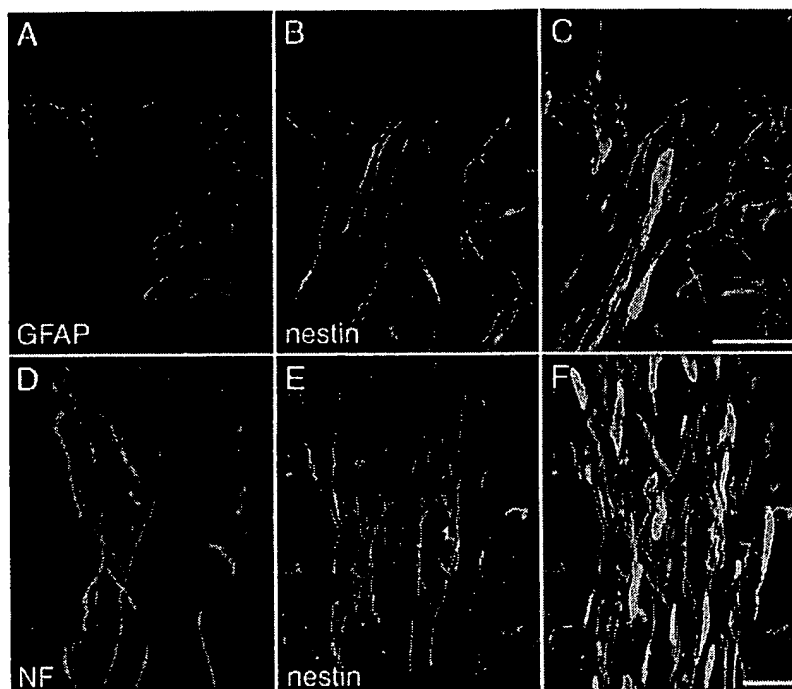
Fig. 5. MSC bundles guide host neuropil. (A–C) Beyond the astrocytic scar surrounding the epicenter of the lesion (A), nestin-positive (blue) and GFAP-negative immature astrocytes (B) are found closely associated with transplanted MSC (C). (D–F) Neurofilament-IR fibers (red) are found in close relationship with nestin-IR fibers (blue) mainly in the periphery of MSC bundles. (Bars = 25 μm.)

106, $n = 8$) (unpaired t test; $P = 0.0052$). MSC infused immediately after SCI were found mainly in the periphery of the injury zone, whereas MSC transplanted 1 week after SCI were found in the whole lesion zone (Fig. 4A). Implanted MSC exhibited a bipolar morphology with long processes extending along the axis of the spinal cord. MSC formed bundles, which were arranged mainly along the long axis of the spinal cord, and provided bridges across the epicenter of the lesion area, which was filled with debris and macrophages. All implanted MSC expressed fibronectin-IR and a weak but distinct NeuN-IR (ref. 31, Fig. 5, and Table 1). Interestingly, implanted MSC had lost detectable nestin-IR (Fig. 4B and Fig. 6) as well as vimentin and laminin-IR (Table 1). Nestin and GFAP antibodies revealed the presence of two different kinds of glial cells in the injured spinal cord. GFAP and nestin-positive reactive astrocytes delineated the margin of the epicenter of the lesion with their tightly interwoven processes. In animals that had received a MSC infusion, astrocytic processes reached into the epicenter by

Fig. 6. (A and B) Five weeks after SCI, MSC express a distinct nuclear NeuN-IR. (C) All MSC are fibronectin-positive. [Bar = 10 μm (A) and 25 μm (B and C).]

penetrating MSC-bundles (Fig. 4C). A second population of cells was nestin-positive but GFAP-negative and, thus, similar to immature astrocytes (32). These cells had migrated into the epicenter of the injury. In animals treated with MSC, immature astrocytes populated the MSC bundles and extended their delicate processes along the engrafted cells (Fig. 4B and Fig. 5 A–C). NF-positive fibers were preferentially found at the interface between MSC bundles and scar tissue (Fig. 4E and Fig. 5 D–F). Some of the nerve fibers associated with the implanted cells were identified as 5-HT-positive (Fig. 4D). The intraspinal MSC did not display GFAP, NF, MAP-2, or PGP 9.5 immunoreactivity.

Discussion

Our results further characterize MSC and demonstrate that MSC treatment can improve recovery of animals rendered paraplegic by SCI. Engrafted MSC form bundles and guide regenerating neuropil through the spinal cord lesion.

MSC grown out of marrow cell suspensions by selective attachment to tissue culture plastic initially are not homogeneous but become morphologically more homogeneous with time in culture (33) by depletion of hematopoietic cells. However, the relationship between hematopoietic stem cells and marrow stromal cells is the topic of intensive research (34). When neonatal mice incapable of developing cells of the myeloid and lymphoid lineages were transplanted with whole bone marrow fractions from healthy donors, bone marrow-derived cells expressing NeuN and NSE were found within the central nervous system (35). In a similar experiment, adult irradiated mice were infused with a whole bone marrow fraction. Cells engrafted in the olfactory bulb were immunoreactive for NeuN, NF, and Tuj1 (36). However, these experiments did not determine whether the bone marrow-derived cells detected in the brain were derived from mesenchymal or hematopoietic stem cells. For our experiments, we used long-term MSC cultures containing mesenchymal stem cells selected on the basis of adherence to plastic. With the exception of a weak NeuN-IR seen in intraspinal MSC, neither neuronal induction *in vitro* nor environmental cues
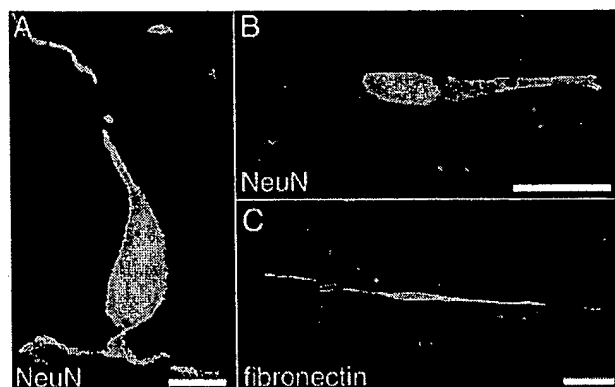
provided by the injured spinal cord *in vivo* could differentiate the MSC toward a neuronal fate, suggesting that cells with more developed neuronal characteristics detected by other groups are of hematopoietic origin.

By using confocal microscopy, reliable colocalization of markers expressed by the GFP-labeled cells was possible. In culture, conditions all MSC displayed fibronectin, vimentin, and laminin-IR. Interestingly, a subpopulation of MSC expressed nestin, which is expressed during early stages of neurogenesis (37) and myogenesis (38). Attempts were made to differentiate marrow stromal cells toward a neuronal fate. In addition to the two induction media published here, we tested media containing retinoic acid, brain-derived neurotrophic factor (21), nerve growth factor, NT-3, glial cell line-derived neurotrophic factor (GDNF), and forskolin (unpublished data). However, none of these supplements improved the neuronal differentiation of MSC. Considering that differentiation of MSC into myoblasts has been reported (19), it could be possible that the nestin-positive subpopulation of MSC differentiates spontaneously into an early myoblastic state during culture conditions. Five weeks after transplantation into the injured spinal cord, MSC had down-regulated vimentin, laminin, and nestin and begun to express a weak nuclear NeuN-IR, indicating that they had been instructed by environmental cues present in the injured spinal cord. Importantly, transplanted MSC formed bundles bridging the epicenter of the lesion filled with debris and macrophages. Regenerating host neuropil was associated with MSC aggregates, and, thus, a degree of cellular organization had been reestablished in the injury zone. Immature astrocytes, defined as nestin-positive and GFAP-negative cells, which are formed from stem cells in response to injury (32), populated the MSC bundles. These cells might help promote nerve fiber outgrowth by offering a growth-permissive surface. Growth of nerve fibers on the surface of astrocytes has been observed in other studies in which peripheral nerves (39) or fibroblasts secreting NGF (40) were

implanted. Another explanation for the guidance of nerve fibers might be the abundant expression of *N*-cadherin (41), which is known to enhance neurite extension (42), on the surface of MSC. Importantly, we identified 5-HT-positive nerve fibers along the MSC bundles. The 5-HT-system of the spinal cord has been shown to be important in functional recovery after SCI (43, 44), and the apparent regeneration of 5-HT elicited by MSC thus may be contributing to the observed improvement of behavioral recovery. From a clinical standpoint, it is perhaps particularly encouraging that delayed MSC treatment enhanced survival of grafted cells and exerted a beneficial effect on functional recovery. MSC infused immediately after SCI encounter a hostile environment characterized by ischemia, necrosis, and the presence of potentially toxic compounds such as oxygen radicals and lytic enzymes. However, 12 h after SCI, maximal tissue loss is reached, leading to the next phase characterized by reactive gliosis, invasion of inflammatory cells, and reparative attempts such as up-regulation of basic fibroblast growth factor. Our data are indicating that this later phase of SCI is providing a more habitable environment for infused cells. Autologous treatment thus might become possible, avoiding graft rejection, the risk of viral antigens, and possible ethical concerns associated with other sources of stem cells.

In summary, our results demonstrate that MSC survive well in the contused and severely pathological tissue present in the lesion after SCI and form physical, nerve fiber-permissive tissue bridges across areas of debris that are associated with a degree of long-term functional improvement.

1. Fawcett, J. W. & Asher, R. A. (1999) *Brain Res. Bull.* 49, 377–391.
2. Skene, J. H. (1989) *Annu. Rev. Neurosci.* 12, 127–156.
3. Widenfalk, J., Lundstromer, K., Jubran, M., Brene, S. & Olson, L. (2001) *J. Neurosci.* 21, 3457–3475.
4. Schwartz, M. (2000) *Prog. Brain Res.* 128, 259–263.
5. Schnell, L. & Schwab, M. E. (1990) *Nature (London)* 343, 269–272.
6. Merkler, D., Metz, G. A., Raineteau, O., Dietz, V., Schwab, M. E. & Fouad, K. (2001) *J. Neurosci.* 21, 3665–3673.
7. McKerracher, L., David, S., Jackson, D. L., Kottis, V., Dunn, R. J. & Braun, P. E. (1994) *Neuron* 13, 805–811.
8. Becker, T., Anliker, B., Becker, C. G., Taylor, J., Schachner, M., Meyer, R. L. & Bartsch, U. (2000) *Glia* 29, 330–346.
9. Lemons, M. L., Howland, D. R. & Anderson, D. K. (1999) *Exp. Neurol.* 160, 51–65.
10. Yoles, E., Hauben, E., Palgi, O., Agranov, E., Gothilf, A., Cohen, A., Kuchroo, V., Cohen, I. R., Weiner, H. & Schwartz, M. (2001) *J. Neurosci.* 21, 3740–3748.
11. Davies, S. J., Fitch, M. T., Memberg, S. P., Hall, A. K., Raisman, G. & Silver, J. (1997) *Nature (London)* 390, 680–683.
12. McDonald, J. W., Liu, X. Z., Qu, Y., Liu, S., Mickey, S. K., Turetsky, D., Gottlieb, D. I. & Choi, D. W. (1999) *Nat. Med.* 5, 1410–1412.
13. Clark, B. R. & Keating, A. (1995) *Ann. N.Y. Acad. Sci.* 770, 70–78.
14. Azizi, S. A., Stokes, D., Augelli, B. J., DiGirolamo, C. & Prockop, D. J. (1998) *Proc. Natl. Acad. Sci. USA* 95, 3908–3913.
15. Colter, D. C., Class, R., DiGirolamo, C. M. & Prockop, D. J. (2000) *Proc. Natl. Acad. Sci. USA* 97, 3213–3218.
16. Schwarz, E. J., Alexander, G. M., Prockop, D. J. & Azizi, S. A. (1999) *Hum. Gene Ther.* 10, 2539–2549.
17. Beresford, J. N., Bennett, J. H., Devlin, C., Leboy, P. S. & Owen, M. E. (1992) *J. Cell Sci.* 102, 341–351.
18. Lennon, D. P., Haynesworth, S. E., Young, R. G., Dennis, J. E. & Caplan, A. I. (1995) *Exp. Cell Res.* 219, 211–222.
19. Wakitani, S., Saito, T. & Caplan, A. I. (1995) *Muscle Nerve* 18, 1417–1426.
20. Woodbury, D., Schwarz, E. J., Prockop, D. J. & Black, I. B. (2000) *J. Neurosci. Res.* 61, 364–370.
21. Sanchez-Ramos, J., Song, S., Cardozo-Pelaez, F., Hazzi, C., Stedeford, T., Willing, A., Freeman, T. B., Saporta, S., Janssen, W., Patel, N., *et al.* (2000) *Exp. Neurol.* 164, 247–256.
22. Deng, W., Obrocka, M., Fischer, I. & Prockop, D. J. (2001) *Biochem. Biophys. Res. Commun.* 282, 148–152.
23. Kopen, G. C., Prockop, D. J. & Phinney, D. G. (1999) *Proc. Natl. Acad. Sci. USA* 96, 10711–10716.
24. Miller, A. D. & Rosman, G. J. (1989) *BioTechniques* 7, 980–990.
25. Kinsella, T. M. & Nolan, G. P. (1996) *Hum. Gene Ther.* 7, 1405–1413.
26. Gruner, J. A. (1992) *J. Neurotrauma* 9, 123–128.
27. Basso, D. M., Beattie, M. S. & Bresnahan, J. C. (1995) *J. Neurotrauma* 12, 1–21.
28. Abercrombie, M. (1946) *Anat. Rec.* 94, 239–247.
29. Hökfelt, T., Fuxe, K., Goldstein, M. & Johansson, O. (1973) *Acta Physiol. Scand.* 89, 286–288.
30. Dahl, D. & Bignami, A. (1977) *J. Comp. Neurol.* 176, 645–657.
31. Chopp, M., Zhang, X. H., Li, Y., Wang, L., Chen, J., Lu, D., Lu, M. & Rosenblum, M. (2000) *NeuroReport* 11, 3001–3005.
32. Johansson, C. B., Momma, S., Clarke, D. L., Risling, M., Lendahl, U. & Frisen, J. (1999) *Cell* 96, 25–34.
33. Bruder, S. P., Jaiswal, N. & Haynesworth, S. E. (1997) *J. Cell Biochem.* 64, 278–294.
34. Huss, R. (2000) *J. Hematother. Stem Cell Res.* 9, 783–793.
35. Mezey, E., Chandross, K. J., Harta, G., Maki, R. A. & McKercher, S. R. (2000) *Science* 290, 1779–1782.
36. Brazelton, T. R., Rossi, F. M., Keshet, G. I. & Blau, H. M. (2000) *Science* 290, 1775–1779.
37. Lendahl, U., Zimmerman, L. B. & McKay, R. D. (1990) *Cell* 60, 585–595.
38. Sejersen, T. & Lendahl, U. (1993) *J. Cell Sci.* 106, 1291–1300.
39. Campbell, G., Lieberman, A. R., Anderson, P. N. & Turmaine, M. (1992) *J. Neurocytol.* 21, 755–787.
40. Kawaja, M. D., Ray, J. & Gage, F. H. (1991) *Genet. Eng.* 13, 205–220.
41. Puch, S., Armeanu, S., Kibler, C., Johnson, K. R., Muller, C. A., Wheelock, M. J. & Klein, G. (2001) *J. Cell Sci.* 114, 1567–1577.
42. Schense, J. C., Bloch, J., Aebischer, P. & Hubbell, J. A. (2000) *Nat. Biotechnol.* 18, 415–419.
43. Bregman, B. S., Kunkel-Bagden, E., Reier, P. J., Dai, H. N., McAtee, M. & Gao, D. (1993) *Exp. Neurol.* 123, 3–16.
44. Nygren, L. G., Fuxe, K., Jonsson, G. & Olson, L. (1974) *Brain Res.* 78, 377–394.